Selected Papers of The Society of Naval Architects of Korea, Vol.1, 1993, pp. 91~100.

# Geometrically Nonlinear Analysis of Eccentrically Stiffened Plates

Jae Wook Lee*, Kie Tae Chung** and Young Tae Yang***

(From T.S.N.A.K., Vol.28, No.2, 1991)


## Abstract

A displacement-based finite element method is presented for the geometrically nonlinear analysis of eccentrically stiffened plates.

A nonlinear degenerated shell element and a nonlinear degenerated eccentric isoparametric beam (isobeam) element are formulated on the basis of Total Agrangian and Updated Lagrangian descriptions. In the formulation of the isobeam element, some additional local degrees of freedom are implementd to describe the stiffener's local plate buckling modes. Therefore this element can be effectively employed to model the eccentric stiffener with fewer D.O.F's than the case of a degenerated shell element.

Some detailed buckling and nonlinear analyses of an eccentrically stiffened plate are performed to estimate the critical buckling loads and the post buckling behaviors including the local plate buckling of the stiffeners discretized with the degenerated shell elements and the isobeam elements. The critical buckling loads are found to be higher than the analytical plate buckling load but lower than Euler buckling load of the corresponding column, i.e, buckling strength requirements of the Classification Societies for the stiffened plates.


## 1. Introduction

It is very important to verify the structural stability criteria of the eccentrically stiffened plates which are basic structural components of ship and offshore structures, because the loss of stability can result in catastrophic failures of total structures.

It has been well recongnized that for the eccentrically stiffened plates the quantitative verifications of structural stability and post-buckling analyses considering the geometrical form of the stiffeners are more and more required, as the sizes of structures become larger[1,2,12,17].

In today's practice the structural analysis programs such as SAP, ADINA, NASTRAN, and others are used to analyze the buckling strength of stiffened plates by modeling stiffeners with

* Inha University
** Choongnam National University
*** Hyundai Heavy Industry

beam elements with offsets to consider their eccentricities. Modeling the stiffeners with beam elements, however, it is impossible to assess the possibility of the local plate buckling of the stiffener's web or flange occurring prior to the column buckling of a stiffened plate. Of course it is possible to model the stiffeners and the plate with plate elements together to investigate the local plate buckling, if suffering the excessively large D.O.F's required. Therefore it has been required to develop a special beam element, which can consider the eccentricity and the local plate buckling behaviors of a stiffener[12,14]

Since Ahmand has introduced the degeneration concept in describing the geometrical motion of a continuum as that of the reference line or the reference plane, many kinds of degenerated elements have been successfully developed and used to investigate the geometrical or material nonlinear analyses[3-16].

In this paper the degenerated shell element and the degenerated eccentric isobeam element have been developed and used to idealize the eccentrically stiffened plate, in which Total Lagrangian (T.L.) and Updated Lagrangian (U.L.) formulations are carefully tested to investigate the nonlinear behaviors of the degenerated elements.

Numerical iterations in nonlinear analyses are carried out with new Modified Arc Length Method or Cylindrical Arc Length Method, which is one of the revised Newton-Raphson iteration schemes originally proposed by Riks.

## 2. Finite Element Formulation

### 2.1 Degenerated shell element

2.1.1 Displacement

As shown in Fig.1, the geometrical shape of a degenerated shell element can be described with nodal coordinates and directional vectors at nodes on the mid-surface of an element. The nodal behavior can be described with 3 displacements vectors ($U_i$, $i=1,2,3$) in global rectangular coordinates and 3 directional vectors ($V_{ni}$, $i=1,2,3$)

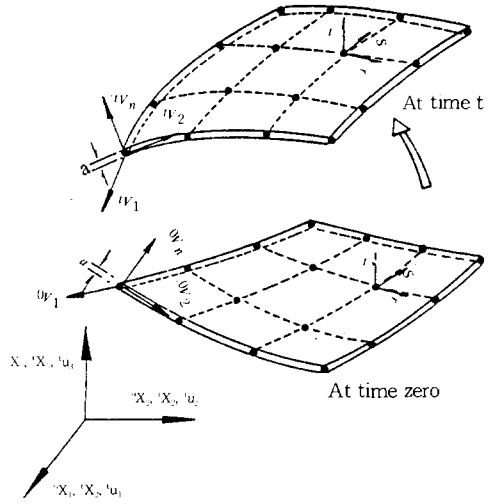


Fig.1 Degenerated shell element undergoing large displacements and rotations

in local curvilinear coordinates[3-16]. The geometrical shape of an element at time t can be written with the nodal coordinates as follows.

$$ {}^{t}X_i = \sum_{k=1}^{N} h^k(r,s)\,{}^{t}X_i^k + \frac{t}{2}\sum a_k h^k(r,s)\,{}^{t}V_{ni}^k \qquad (1) $$

${}^{t}X_i$ : rectangular coordinates of a point on an element at time t

${}^{t}X_i^k$ : rectangular coordinates of k-th node at time t

$h^k(r,s)$ : interpolation functions of 2nd or 3rd order of k-th node in r-s plane

${}^{t}V_{ni}^k$ : unit directional vectors of k-th node normal to the mid-surface

The incremental displacements and the corresponding nodal normal vectors are defined as follows.

$$ U_i = \sum_{k=1}^{N} h^k(r,s)U_i^k + \frac{t}{2}\sum_{k=1}^{N} a_k h^k(r,s)V_{ni}^k \qquad (2) $$

$$ V_{ni}^k = {}^{t+dt}V_{ni}^k - {}^{t}V_{ni}^k \qquad (3) $$

In the equation (3) ${}^tV_{ni}^k$ can be described as the trigonometrical functions using the rotational angles between the nodal normal vector and the coordinates ${}^tX_i^k$ and the incremental rotations $\alpha^k$, $\beta^k$. Assuming that $\alpha^k$ and $\beta^k$ are small and taking the linear terms from series expansions of trigonometrical functions, the unit normal vectors and the incremental displacements can be rewritten as follows.

$$V_{ni}^k = {}^tF_{i1}^k\,\alpha^k + {}^tF_{i2}^k\beta^k \tag{4}$$

$$U_i = \sum_{k=1}^{N} h^k(r,s)U_i^k + \frac{t}{2}\sum_{k=1}^{N} a_k h^k(r,s)[{}^tF_{i2}^k][{}^{\alpha}_{\beta}{}^k] \tag{5}$$

In order to describe the strain-deflection relations in global coordinates, the partial derivatives of incremental displacements to the global coordinates can be defined using the Jacobian matrix after the derivation of the partial derivatives of incremental displacement to the local coordinates. In T.L. and U.L. formulations the Jacobian matrices are defined in the initial configuration and in the deformed configuration as follows.

$$\left(\frac{\partial U}{\partial {}^mX}\right) = {}^mJ^{-1}\left(\frac{\partial U}{\partial R}\right) \tag{6}$$

$T.L: m = 0$

$U.L.: m = t$

$$\left[\frac{\partial U_i}{\partial {}^mX_i}\right]^k = \sum_{k=1}^{N}\left[{}^mJ_{j1}^{-1}\frac{\partial U_i}{\partial r} + {}^mJ_{j2}^{-1}\frac{\partial U_i}{\partial s} + {}^mJ_{j3}^{-1}\frac{\partial U_i}{\partial t}\right]^k \tag{7}$$

2.1.2 Stress-strain relations

The strain-displacement matrix B can be defined by using equation (7). The incremental linear strain ${}^te$ and the incremental nonlinear strain ${}^td$ can be defined as follows.

$${}_me = {}^{l}_{m}B_L U \tag{8}$$

$${}_md = {}^{l}_{m}B_{NL} U_L \tag{9}$$

Following the assumptions of a degenerated shell element, the stress component normal to the mid-surface can be disregarded and the 2nd Piola-Kirchhoff incremental stress and the Green-Lagrange incremental strain can be defined as the following equation.

$${}_mS = {}_mC\ {}_me \tag{10}$$

$${}_mC = G^T\,C'\,G \tag{11}$$

, where the $G$ is the transformation matrix between the global and local curvilinear coordinates.

### 2.2 Degenerated isobeam element

2.2.1 Displacement

In the formulation of the degenerated isobeam element the interpolation functions of 2nd or 3rd order are to be taken of same order as those of degenerated shell elements to satisfy compatibility between two elements. The geometrical shape of a degenerated isobeam element is shown in Fig.2 and the coordinates of a point in an element can be written as follows[9-15].

$${}^tX_i = \sum_{k=1}^{N} h^k(r)\,{}^tX_i^k + \sum_{k=1}^{N} h^k(r)(a^k/2\cdot s + e_{ak})\,{}^tV_{si}^k + \sum_{k=1}^{N} h^k(r)(b^k/2\cdot t + e_{bk})\,{}^tV_{ti}^k \tag{12}$$

$h^k(r)$ : interpolation functions of 2nd or 3rd order in r-direction

${}^tV_{si}^k$ : normal vectors of k-th node at time t in s-direction

${}^tV_{ti}^k$ : normal vectors of k-th node at time t in t-direction

$a^k, b^k$ : height and breadth of a beam at k-th node

$e_{ak}, e_{bk}$ : eccentricity of a beam at k-th node

$r,s,t$ : local curvilinear coordinates in an element

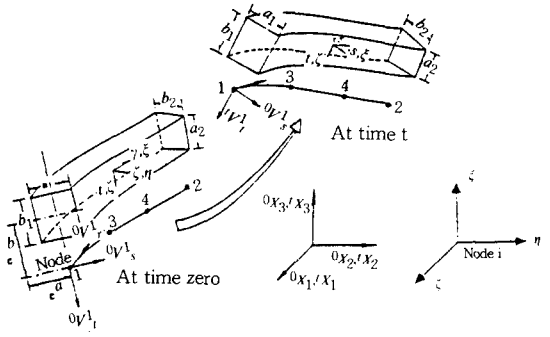


Fig. 2 Degenerated isobeam element undergoing large displacements and rotations

The coordinates $(\xi,\eta,\zeta)$ Fig.2, parellel to the local curvilinear coordinates (r,s,t), are the material local coordinates to define stresses and strains of an isobeam element. They can describle the warping and local plate buckling of the stiffener. The relationship between two local coordinate systems can be defined as follows.

$$\begin{aligned} &\xi_{,r}^2 = X_{,r}^2 + X_{,r}^2 + Z_{,r}^2 \qquad \xi_{,s}=0 \quad \xi_{,t}=0 \\ &\eta_{,r}=0 \qquad\qquad \eta_{,s}=a/2 \quad \eta_{,t}=0 \\ &\zeta_{,r}=0 \qquad\qquad \zeta_{,s}=0 \quad \zeta_{,t}=b/2 \end{aligned} \tag{13}$$

The displacements of a degenerated isobeam element can be divided into the global and local displacements, which describes the warping and the local plate buckling of a beam. The incremental displacements and the corresponding nodal normal vectors at time 0, t and $t^{+}dt$ can be written as the equation (14) and (15).

$$\begin{aligned} {}^{t}U_{gi} = &\sum_{k=1}^{N} h^k(r)\,{}^{t}U_i^k + \sum_{k=1}^{N} h^k(r)(a^k/2 \cdot s - e_{ak})V_{si}^k \\ &+ \sum_{k=1}^{N} h^k(r)(b^k/2 \cdot t + e^{bk})V_{ti}^k \end{aligned} \tag{14}$$

$$\begin{aligned} V_{si}^k &= {}^{t+dt}V_{si}^k - {}^{t}V_{si}^k \\ V_{ti}^k &= {}^{t+dt}V_{ti}^k - {}^{t}V_{ti}^k \end{aligned} \tag{15}$$

The partial derivatives of $U_{gi}$ to the global coordinate can be written in terms of their partial derivatives to the local curvilinear coordinates using Jacobian matrix as follows.

$$\left(\frac{\partial U_g}{\partial {}^{m}X}\right) = {}^{m}J^{-1}\left(\frac{\partial U_g}{\partial R}\right) \tag{16}$$

, where $m=0$ by T.L. and $m=t$ by U.L. formulations.

The equation (16) can be rewritten in local curvilinear coordinates as in equation (18) using the transformation relation in equation (17).

$$({}^{m}X) = ({}^{m}\theta)({}^{m}\xi) \tag{17}$$

$$\begin{aligned} \left(\frac{\partial U\xi}{\partial \xi}\right) &= ({}^{m}\theta)^T\left(\frac{\partial U_g}{\partial {}^{m}X}\right)({}^{m}\theta) \\ &= ({}^{m}\theta)^T\,{}^{m}J^{-1}\left(\frac{\partial U_g}{\partial {}^{m}r}\right)({}^{m}\theta) \end{aligned} \tag{18}$$

2.2.2 Local displacement

(a) Torsional mode

The axial displacement due to warping of a beam subjected to torsions can be described in equation (19) using the local shape functions such as the linear function $f_1(s,t)=st$ and the nonlinear function $f_2(s,t)=s^3t-st^3$ as shown in Fig.3 [12,15]. Incremental axial displacements can be written as follows.

$$U_{\xi T} = \sum_{k=1}^{N} h^k(r)\,\psi_1^k f_1^k(s,t) + \sum_{k=1}^{N} h^k(r)\psi_2^k f_2^k(s,t) \tag{19}$$

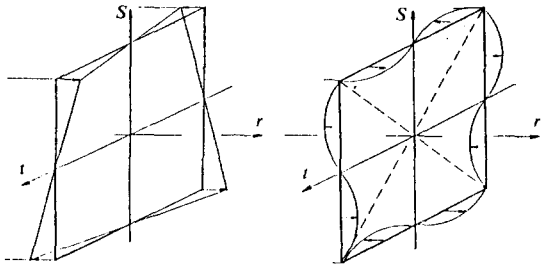


a) $f_1(s,t)=st$ a) $f_1(s,t)=s^3t-st^3$

Fig.3 Shape functions for warping modes

(b) Local plate buckling mode

If the web of the beam is thin as in Fig.4, the web plate buckling can be occurred before the column buckling. In order to describe the local plate buckling of the stiffener, the incremental displacements of the web plate are written as equation (20-22) using the interpolation functions of 2nd or 3rd order in s-t plane section and the longitudinal ones as shown in Fig.5 [12].

$$U_{\eta p}=\sum_{k=1}^{N} h^k(r)\,\psi_3^k(t+\Delta)^2+\sum_{k=1}^{N} h^k(r)\,\psi_4^k(t+\Delta)^3 \quad (20)$$

$$U_{\zeta p}=-\sum_{k=1}^{N} h^k(r)\,\psi_3^k(t+\Delta)^2(a^k/\,b^k)2s - \sum_{k=1}^{N} h^k(r)\,\psi_4^k(t+\Delta)^3(a^k/\,b^k)3s \quad (21)$$

$$U_{\xi p}=+\sum_{k=1}^{N} h^k(r)\,\psi_5^k(t+\Delta)^2(a^k/\,2)s + \sum_{k=1}^{N} h^k(r)\,\psi_6^k(t+\Delta)^3(a^k/\,2)s \quad (22)$$

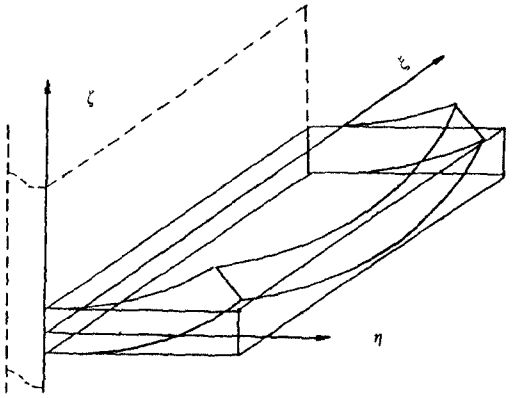


Fig.4 Local plate buckling mode of a stiffener

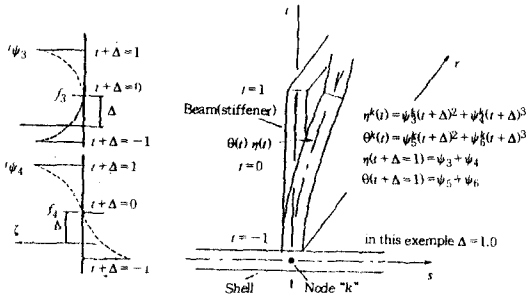


Fig.5 Shape functions for local plate bucking mode

where Δ indicates the location where the local buckling mode is zero. For example Δ is ±1.0 according to the attached positions of the stiffener. Local incremental displacements in a local coordinate system can be obtained by using the relationships in a equation (13) after deriving the partial derivatives to the local curvilinear coordinate as follows.

$$\frac{\partial U\xi_i}{\partial \xi}=\frac{\partial U\xi_i}{\partial r}\cdot\frac{\partial r}{\partial \xi}$$

$$\frac{\partial U\xi_i}{\partial \eta}=\frac{\partial U\xi_i}{\partial s}\cdot\frac{\partial s}{\partial \eta}=\frac{\partial U\xi_i}{\partial s}\cdot(2/a) \quad (23)$$

$$\frac{\partial U\xi_i}{\partial \zeta}=\frac{\partial U\xi_i}{\partial t}\cdot\frac{\partial t}{\partial \zeta}=\frac{\partial U\xi_i}{\partial t}\cdot(2/b)$$

, where the coordinate transformation with respect to the local D.O.F($\psi_i$) is needed at time step $t-1$ in U.L. formulation.

$$^{t}\psi_i = {}^{t}_{t-1}R \;\; {}^{t-1}\psi_i$$

$$^{t}_{t-1}R = \begin{bmatrix} Cos(^{t-1}V_r,\, ^{t}V_r) & 0 & 0 \\ 0 & Cos(^{t-1}V_s,\, ^{t}V_s) & 0 \\ 0 & 0 & Cos(^{t-1}V_s,\, ^{t}V_s) \end{bmatrix} \quad (24)$$

2.2.3 Stress-strain relations

Calculated separately from the global and the local displacements on the basis of the local coordinates, using the equations (18) and (23), the stain-displacement matrix $B$ can be obtained and then the incremental strain can be written separately from the global and local displacements as follows.

$$_{m}e^{g}={}^{t}_{m}B^{g}_{L}U^{g} \qquad {}_{m}e^{gT}=[e_{\xi\xi}\;\; e_{\eta\xi}\;\; e_{\xi\zeta}\;\; 0]$$

$$_{m}e^{1}={}^{t}_{m}B^{1}_{L}U^{1} \qquad {}_{m}e^{gT}=[e_{\xi\xi}\;\; e_{\eta\xi}\;\; e_{\xi\zeta}\;\; e_{\zeta\zeta}]$$

$$^{t}_{m}U^{g}_{k,l}={}_{m}d^{g}={}^{t}_{m}B^{g}_{NL}\,{}_{m}U^{g} \qquad {}_{m}U^{gT}=[U_i \;\; V_{si} \;\; V_{ti}]$$

$$^{t}_{m}U^{1}_{k,l}={}_{m}d^{1}={}^{t}_{m}B^{1}_{NL}\,{}_{m}U^{1} \qquad {}^{m}U^{1T}=[\psi_1\;\psi_2\;\psi_3\;\psi_4\;\psi_5\;\psi_6] \quad (25)$$

$$_{m}e={}^{t}_{m}B_{L}U=\begin{bmatrix} B^{g}_{L} & {}^{t}_{m}B^{1}_{L}\end{bmatrix}\begin{bmatrix} {}_{m}U^{g} \\ {}_{m}U^{1}\end{bmatrix} \quad (26)$$

$$_{m}d={}^{t}_{m}B_{L}U=\begin{bmatrix} B^{g}_{NL} & {}^{t}_{m}B^{1}_{NL}\end{bmatrix}\begin{bmatrix} {}_{m}U^{g} \\ {}_{m}U^{1}\end{bmatrix}$$

, where the incremental strain $e_{\zeta\zeta}$ describing the local plate buckling behavior causes the axial bending stress, $\sigma_{\zeta\zeta}$ and the relation between the 2nd Piola-Kirchhoff incremental stress and the Green-Lagrange strain can be defined as follows.

$$ {}_mS = {}_mC \cdot {}_me \tag{27}$$

### 3. Numerical results

Buckling and post-buckling analyses of stiffened plates are carried out by using degenerated shell elements and degenerated isobeam elements. A numerical model adoped in this paper is shown in Fig.6 and it is idealized in two different models. The first model is called PLPL, in which the plates and the stiffeners are modeled with degenerated shell elements. The second is called PLIB, in which the stiffeners are discretized with the degenerated isobeam elements. The number of elements, nodes and D.O.F's are listed in Table 1. The buckling analyses are carried out at time step 2 and their results are listed in Table 2.

In order to investigate the post-buckling behavior, a nonlinear analysis has been carried out up to time step 100. The load-deflection curves at points A, B and C in Fig.6 are shown in Fig.9 to Fig.14.

Specially in Fig.14 the required buckling requirements of Classification Society, which is 343.0 N/mm$^2$ (Load factor=50.0) for a simply

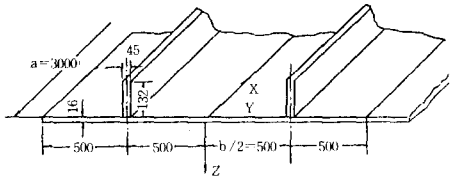


Dimensions of stiffened plate

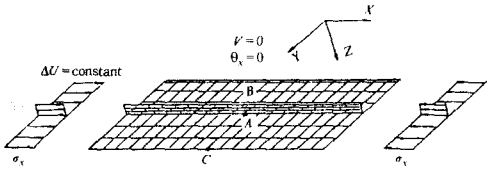


Geometric boundary condition

Fig.6 Eccentrically stiffened plate

Table 1 F.E model of eccentrically stiffened plate

| Model | Plate | Stiffner | Node/dof |
|---|---|---|---|
| PLPL | Deg. shell elements<br>16 nodes<br>10 elements | Deg. shell elements<br>16 nodes<br>5 elements | 160/786 |
| PLIB | Deg. shell elements<br>16 nodes<br>10 elements | Deg. isbeam elements<br>4 nodes<br>5 elements | 128/517 |

the first mode

the second mode

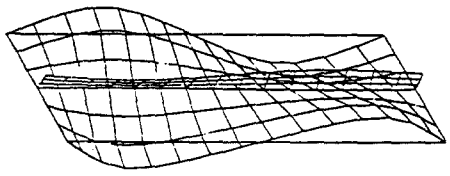

the third mode

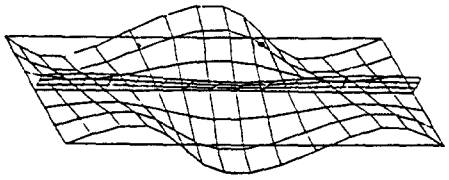

the fourth mode

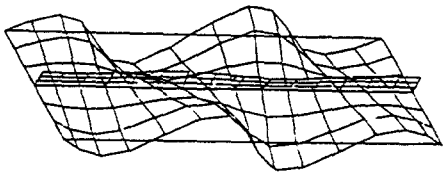

Fig.7 Buckling modes of PLPL model

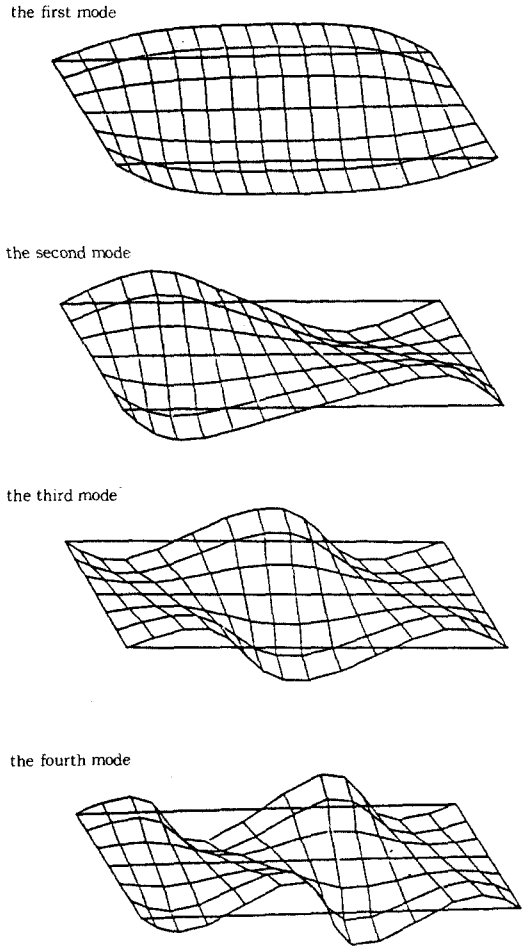


Fig.8 Buckling modes of PLIB model

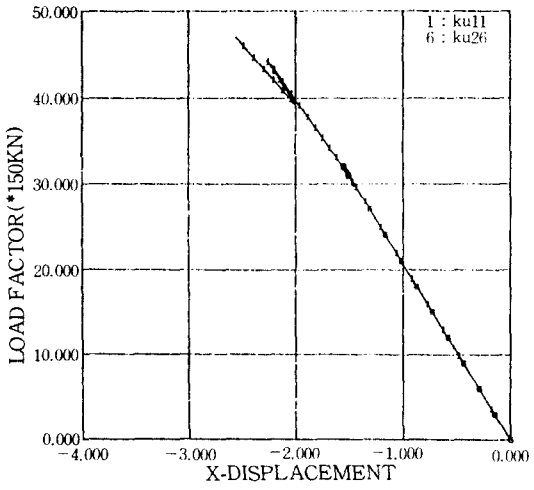


Fig.9 Pre-and post-buckling behavior of node point A in x-direction

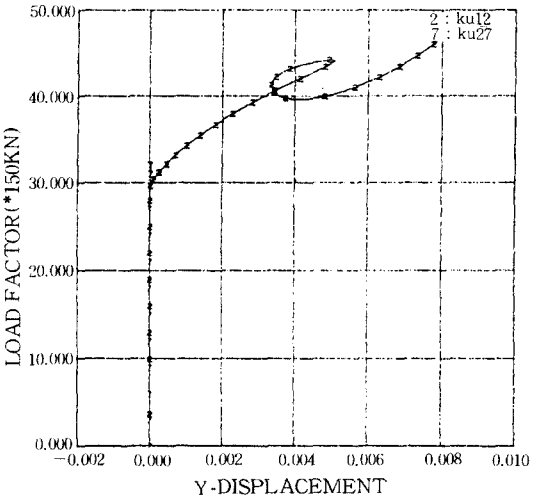


Fig.10 Pre-and post-buckling behavior of node point A in y-direction

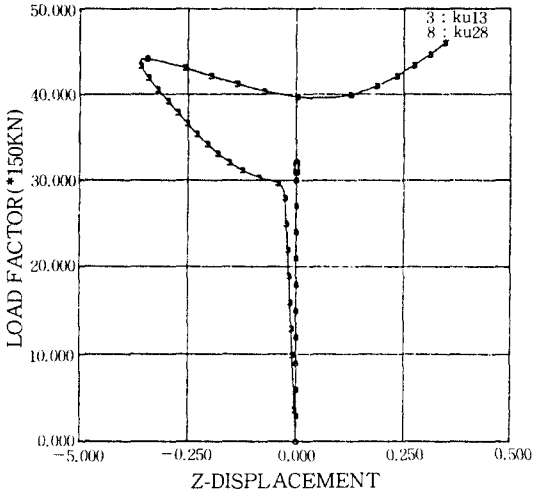


Fig.11 Pre-and post-buckling behavior of node point A in z-direction

supported beam and 194.0 N/mm$^2$ (Load factor = 20.7) for a simply supported plate, are marked together with the load deflection curves from nonlinear analysis. As shown in Fig.9−13 the nodal deflections in x- and y-direction of the PLPL model are same as those of the PLIB model, but the differences of the deflections in z-direction are thought to be originated from the differences of loading situations because of the modeling. When the loads are acting along the free edge of

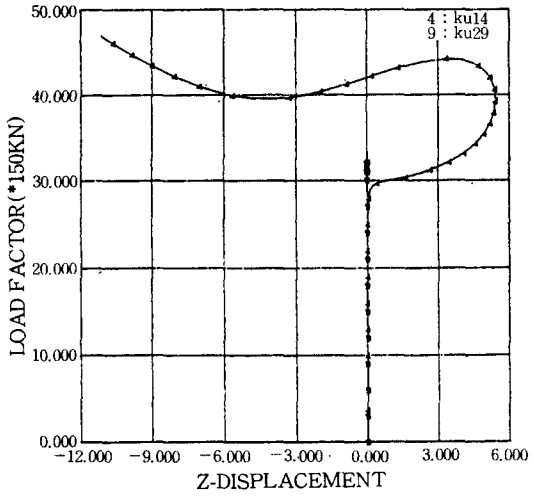


Fig.12 Pre-and post-buckling behavior of node point C in z-direction

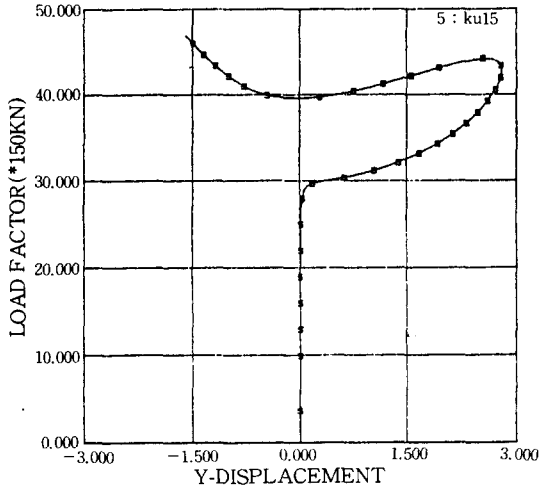


Fig.13 Pre-and post-buckling behavior of node point B in y-direction

the PLPL model, the bending moments are produced due to the eccentric loads acting on the stiffener, which results in larger deflections in z-direction. On the other hand the PLIB model has no large deflections in z-direction because of nonexistance of eccentric loads.

As shown in Fig.15 the PLPL model shows unstable nonlinear behaviors at load factors 10.0 and 44.0 where deformed shapes are consistent with

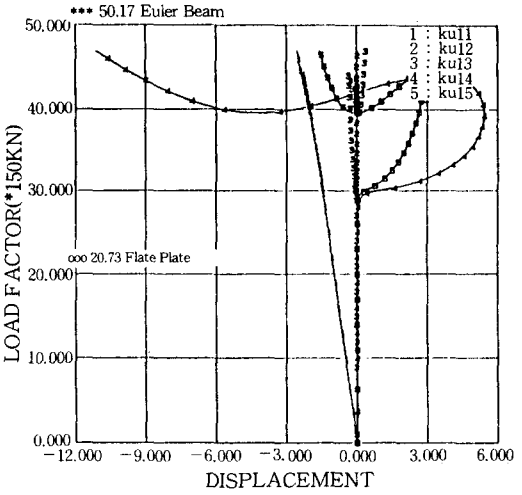


Fig.14 Pre- and post-buckling behavior of node point A, B and C in z-direction

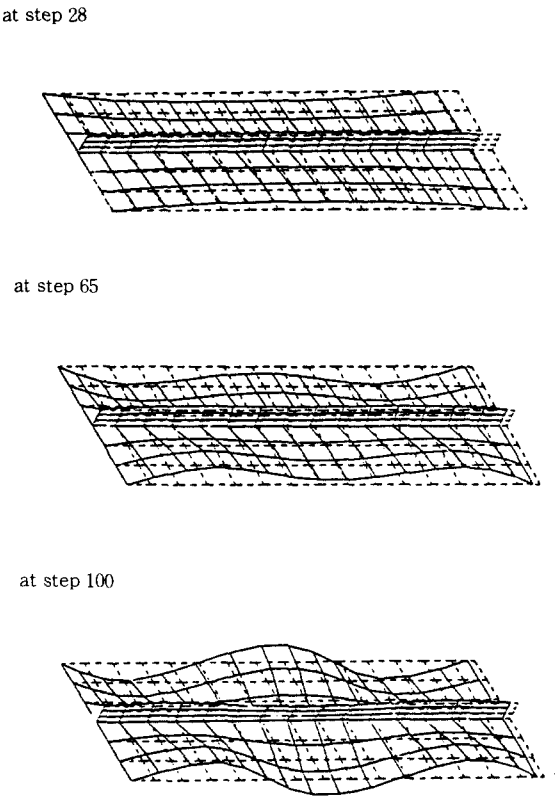


Fig.15 Deformed shapes of PLPL model under axial loads at 3 different various load factors-30.0, 44.0, 47.0

at step 33

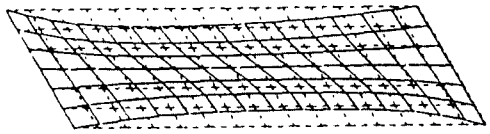

Fig.16 Deformed shape of PLIB model under axial loads at load factor 32.0

those of the 1st and 3rd mode shapes in buckling analyses and it is revealed that the 2nd buckling mode is not shown. It is very interesting to find in Table 2 that the 1st critical stress from two different analysis are same but the 3rd buckling stress is different from that by nonlinear analysis. It is thought that the buckling analysis is performed at time step 2 and the 3rd unstable phenomenon in the nonlinear analysis has begun at time step 65. In Fig.14 the stiffened plate subjected to the compressive loads shows the 1st local plate buckling modes at load factor 30.0 and begins to loss the stiffness and show the overall column buckling mode at load factor 44.0. The stiffness increases after the load factor 39.0.

The PLIB model shows the 1st unstability at load factor 32.0, after which the model shows divergency because of the numerical doubling back. And this model shows relatively small deflection in z-direction at load factor 32.0, because the bending moment due to eccentric loading does not exist. Therefore the deflection in z-direction is, for comparison, amplified and plotted in Fig.16 and it is confirmed that the deformed shape is same as the 1st eigenmode shape and the load factor is consistent with that of eigenvalue analysis as shown in Table 2.

## 4. Conclusions

In order to analyze the geometrical nonlinear behaviors of stiffened plates a nonlinear finite element program with degenerated shell elements and degenerated isobeam elements is developed,

Table 2 Critical buckling stresses

| Model | Critical stress | | | | Remarks |
|---|---|---|---|---|---|
| | 1 | 2 | 3 | 4 | |
| PLPL | 205. | 234. | 245. | 262. | T.L & Eigen. |
| | 210. | 239. | 246. | 264. | U.L & Eigen. |
| | 210. | – | 306. | – | U.L & Non. |
| PLIB | 212. | 239. | 241. | 255. | T.L & Eigen. |
| | 212. | 239. | 242. | 255. | U.L & Eigen. |
| | 214. | – | – | – | U.L & Non. |
| Plate | 194. | | | | * |
| Beam | 343. | | | | ** |

1,2,3,4 : No. of half waves of global and local buckling modes

T.L : Total Lagrangian approach

U.L : Updated Lagrangian approach

Eigen. : Eigen value problem

Non : Nonlinear path approach

* : Euler stress of simply supported plate

** : Euler stress of simply supported beam with full effective breadth

where the Total Lagrange(T.L.) and the Updated Lagrange(U.L.) formulations are implemented combined with the iteration schemes such as the modified normal arc length method or the cylindrical arc length method.

An eccentrically stiffened plate is modeled with two different idealizations, i.e., a PLPL(Plate-Plate) model and a PLIB(Plate-Isobeam) model. The calculation results show that the two models by T.L. and U.L. formulations give the same buckling mode shapes but slightly different stresses by 3.4%. It can be concluded that the degenerated isobeam element can be an efficient element to verify the local plate buckling phenomena of the eccentrically stiffened plate and effectively used to calculate the local plate buckling strength.

In the future the numerical doubling buck in the PLIB model starting at the first critical load may need to be investigated and some experimental studies are also needed to verify the exactness and efficiency of the program developed in this paper. However the numerical results show that the program can be a good tool to analyze the nonlinear behaviors and the buckling for the ec-

centrically stiffened plate structures typically built in ship and offshore structures.

## References


[1] J.W. Lee, K.T. Chung, Y.T. Yang, "Buckling Analysis of Ship Structural Members", (in Korean). I.T.R.I. of Inha Uni., 1989.

[2] J.W. Lee, K.T. Chung, Y.T. Yang, "Study on Buckling Analysis of Stiffened Plates", (in Korean), KRISO, 1989.

[3] Ahmad, S., Irons, B.M. and Zienkiewicz, O.C. "Analysis of Thick and Thin Shell Structures by Curved Finite Elements", Int. J. Num. Eng. Vol.12, 1970, pp.419-451.

[4] Bathe, K.J., Ramm, E. and Willson, E.L. "Finite Element Formulation for Large Deformation Analysis", Int. J. Num. Eng., Vol. 19. pp.351-386, 1975.

[5] Ramm, E. "A Plate/Shell Element for Large Deflection and Rotation, Formulation and Computational Algorithms in Finite Element Analysis", MIT Press, Cambridge, Mass., 1977.

[6] Nukulchai, K.W. "A Simple and Efficient Finite Element for General Shell Analysis", Int. J. Num. Meth. Engng. Vol.14, 1979, pp. 179-200.

[7] Bathe, K.J. and Dvorkin, E. "Our Discrete Kirchhoff and Isoparametric Shell Elements for Nonlinear Analysis, An Assesment", Comp. & Struc. Vol.16, pp.89-98, 1983.

[8] Surana, K.S. "Geometrically Nonlinear Formulation for the Curved Shell Elements", Int. J. Num. Meth. Eng., Vol.19, pp. 581-615, 1983.

[9] Bathe, K.J. and Bolourchi, S. "A Geometric and Material Nonlinear Plate and Shell Element", Comp. & Struc. Vol.11, pp.23-28, 1980.

[10] Bathe, K.J. "Finite Element Procedures in Engineering Analysis" Prentice-Hall, 1982.

[11] Zienkiewicz, O.C., "The Finite Element Method" Third Edition McGraw-Hill, 1982.

[12] Bernhardi, O. "Eine Geometrische Nichtlineare Finite Elemente Formulierung fuer die Idealisierung Exzentrischer Aussteifungen", (in German) Ph.D Thesis, RWTH Aachen, 1985.

[13] Bathe, K.J. and Wiener, P.M. "On Elastic-Plastic Analysis of I-Beams in Bending and Torsion", Comp. & Struc., Vol.17, pp. 711-718, 1983.

[14] Ferguson, G.H. and Clark, R.D. "A Variable Thickness Curved Beam and Shell Stiffening Element with Shear Deformation", Int. J. Num. Meth. Engng. Vol.14, pp.581-592, 1979.

[15] Bathe, K.J. and Chaudhary, A. "On the Displacement Formulation of Torsion of Shafts with Rectangular Cross-Section", Int. J. Num. Meth. Eng. Vol.18, pp.1565-1580, 1982.

[16] Ramm, E. "Geometrishche Nichtlineare Elastotatik and Finite Elemente", Stuttgart Bericht Nr. 76.2, Stuttgaart, 1976.

[17] Ise, G "Analysis of Eccentrically Stiffened Wide Panels", Recent Advances in Nonlinear Computational Mechanics, eds. E. Hinton, D.R.J. Owen, C. Taylor, Swansea, U.K. 1982.